

# Phosphorus-Centered and Phosphinidene-Capped Tungsten Chloride Clusters

Markus Ströbele,<sup>[a]</sup> Klaus Eichele,<sup>[b]</sup> and H.-Jürgen Meyer\*<sup>[a]</sup>

*Dedicated to Professor John D. Corbett on the occasion of his 85th birthday*

**Keywords:** Tungsten / Cluster compounds / Solid-state structures / X-ray diffraction

Black crystalline powders of  $W_6PCl_{17}$  and  $W_4(PCl)Cl_{10}$  were obtained after reducing  $WCl_6$  with red phosphorus at 370 and 500 °C. The crystal structures were determined by single-crystal and powder X-ray diffraction analyses. The structure of  $W_6PCl_{17}$  is represented by a phosphorus-centered hexanuclear tungsten cluster, whose  $(W_6PCl_{11})Cl_4^aCl_{4/2}^{a-a}$  chains form a hexagonal stick packing structure. The struc-

ture of  $W_4(PCl)Cl_{10}$  is represented by a Jahn–Teller distorted tetranuclear tungsten cluster that is interconnected into a layered  $[W_4(\mu_4-PCl)Cl_6^i]Cl_{8/2}^{a-a}$  structure containing a chloro-phosphinidene ligand. Solid-state  $^{31}P$  magic-angle spinning (MAS) NMR spectra, electronic structures, and magnetic properties are reported.

## Introduction

The chemistry of transition-metal clusters is a unique field of chemistry with inherently beautiful cluster motifs, a surprising chemistry in solid state and in solution, and with developing applications. One of the most simple tungsten chloride cluster compounds is  $W_6Cl_{12}$  with an octahedral cluster core, which represents the functional block for its remarkable properties with regard to photoluminescence,<sup>[1]</sup> catalysis,<sup>[2]</sup> and chemical sensing.<sup>[3]</sup>

Besides the polymeric structure of  $W_6Cl_{12}$  {or  $(W_6Cl_8)_i-Cl_2^aCl_{4/2}^{a-a}$ }, there are two molecular-based structures of tungsten chloride clusters, namely *octahedro*- $W_6Cl_{18}$   $\{(W_6Cl_{12})^iCl_6^a\}$ <sup>[4]</sup> and *triprismo*- $W_6CCl_{18}$   $\{(W_6CCl_{12})^i-Cl_6^a\}$ .<sup>[5]</sup> The structure of  $W_6CCl_{18}$  contains a carbon-centered trigonal-prismatic cluster and follows the prototype structure of  $A_3[Nb_6SBr_{17}]$  ( $A = K, Rb, Cs, Tl$ )<sup>[6]</sup> with a sulfur-centered trigonal-prismatic cluster core.

Most tungsten halide clusters like *octahedro*- $[W_6Cl_{18}]^{m-}$  and *triprismo*- $[W_6ZCl_{18}]^{m-}$  with  $Z = C$  or  $N$  can be employed in solution chemistry with variable oxidation states<sup>[7]</sup> and diverse ligands.<sup>[8]</sup>

The synthesis of metal-rich tungsten chlorides is usually performed following the reduction of  $WCl_6$  with electropositive metals; the reduction with aluminium is well-established.<sup>[9]</sup> Recently, the reduction of  $WCl_6$  with the metal bis-

moth has opened up an alternative route for the synthesis of  $W_6Cl_{12}$ .<sup>[10]</sup>

$W_6Cl_{12}$  itself is an attractive starting material for the preparation of other cluster compounds, as shown by oxidation and reduction reactions with carbon halide sources. Various tungsten halide clusters can be obtained, among them the novel compounds  $W_{30}C_2(Cl,Br)_{68}$  and  $W_6CCl_{15}$ .<sup>[11]</sup>

At present, we are exploring the reduction of  $WCl_6$  by using soft reducing agents and moderate heating temperatures (this temperature region is not often used) in order to explore the potentially largest field of missing compounds – the thermally labile cluster compounds.<sup>[12]</sup>

Over the course of systematic investigations with the employment of phosphorus as a reducing agent, we here present the novel cluster compounds  $W_6PCl_{17}$  and  $W_4(PCl)Cl_{10}$ , which represent the first examples of phosphorus-containing tungsten halide clusters. The  $WCl_6$  reduction with elemental red phosphorus has been described before, but obviously under different conditions.<sup>[13,14]</sup>

## Results and Discussion

### Synthesis and Characterization

The phosphorus-centered cluster compound  $W_6PCl_{17}$  is formed as a black microcrystalline powder by reduction of  $WCl_6$  with elemental red phosphorus at around 360–380 °C. The slightly more reduced phosphinidene-capped tetranuclear cluster compound  $W_4(PCl)Cl_{10}$  was obtained at 500 °C and forms black plate-like crystals. The structures of these compounds contain an interstitial phosphido and a capping phosphinidene ligand, which are both known as important and versatile ligands in organic chemistry and as

[a] Institut für Anorganische Chemie, Abteilung für Festkörperchemie und Theoretische Anorganische Chemie, Universität Tübingen, Ob dem Himmelreich 7, 72074 Tübingen, Germany  
E-mail: juergen.meyer@uni-tuebingen.de

[b] Institut für Anorganische Chemie, Universität Tübingen, Auf der Morgenstelle 18, 72076 Tübingen, Germany  
E-mail: klaus.eichele@uni-tuebingen.de

nucleating ligands in metal cluster chemistry. These ligands enhance the structural integrity and stability through their characteristic face-capping coordination capabilities.

The presence of an interstitial phosphorus atom appears to be rare in the chemistry of metal halide clusters, in contrast to the well-known presence of interstitial carbon or nitrogen atoms. The only example known to us is the series of  $(M_2)Zr_6I_{14}P$  ( $M = Rb, Cs$ ) compounds developed by Corbett and co-workers, where the phosphorus atom resides in the center of an octahedral zirconium cluster [ $d_{Zr-P} = 2.432(2)$  and  $2.494(1)$  Å].<sup>[15]</sup>

From a structural point of view, a phosphorus-centered tungsten cluster may be expected to be related to the known carbon-centered *triprismo*- $W_6CCl_{18}$  cluster or to the motive of a centered *octahedro* cluster, known as an empty cluster in  $W_6Cl_{18}$ . Actually, the refined crystal structure of  $W_6PCl_{17}$  can be considered to represent an intermediate cluster species in-between an octahedral and a trigonal-prismatic cluster, having eight short W–W contacts. A comparison of the structures of  $W_6CCl_{18}$ ,  $W_6PCl_{17}$ , and  $W_6Cl_{18}$  is displayed in Figure 1.

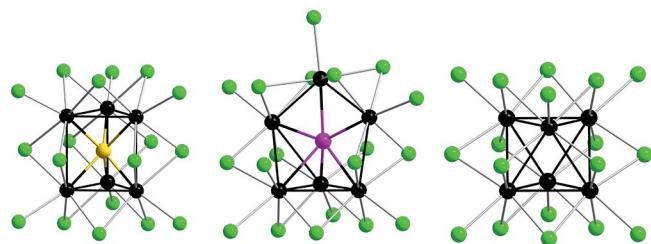


Figure 1. Comparison of structures containing hexanuclear tungsten chloride clusters:  $W_6CCl_{18}$ ,  $W_6PCl_{17}$  {shown as  $(W_6PCl_{19})^{2-}$ }, and  $W_6Cl_{18}$  (from left to right).

Phosphorus-containing clusters are also known in homoleptic alkoxide cluster compounds, such as the trigonal tungsten cluster compound  $W_3(P)(OR)_9$ <sup>[16]</sup> [ $d_{W-P} = 2.365(4)$  Å] and the rhomboidal tungsten cluster compound  $W_4(P)_2(OR)_{10}$  [ $d_{W-P} = 2.292(4)$  to  $2.692(1)$  Å].<sup>[17]</sup> The coordi-

ination mode of the phosphorus atom in these compounds is  $\mu_3$ -capping and the P atom is treated as a phosphido ligand ( $P^{3-}$ ).

When the phosphorus atom in  $W_6PCl_{17}$  is treated in the same way, an electron count of 16 electrons per  $W_6$  core can be assigned. This electron count is consistent with results of an extended Hückel molecular orbital calculation of an isolated  $[W_6PCl_{19}]^{2-}$  cluster. EHMO calculations are known to be inherently semiempirical and qualitative, but show good results in cluster chemistry.<sup>[18]</sup> The total electron count of 176 valence electrons of an isolated  $[W_6PCl_{19}]^{2-}$  cluster is confined in 80 energetically low-lying anionic energy levels (3s and 3p levels of Cl and P) and eight metal-centered energy levels, with a nearly nonbonding HOMO.

Following this assignment of electrons, we note a clear distinction to carbon-centered octahedral metal clusters of the  $[Zr_6CCl_{18}]^{n-}$ -type, where strong interactions between carbon 2s, 2p orbitals and cluster d orbitals yield four bonding energy levels [ $(a_{1g}-a_{1g})^b$ ,  $(t_{1u}-t_{1u})^b$ ] below and four antibonding energy levels [ $(a_{1g}-a_{1g})^*$ ,  $(t_{1u}-t_{1u})^*$ ] above the fermi energy. The total number of bonding cluster states therefore remains the same, whereas the number of valence electrons increases by four electrons by the interstitial carbon atom.

The weakly paramagnetic behavior obtained for  $W_6PCl_{17}$  may be attributed to a very small band gap and the black body color (metallic lustre) of the crystal powder, but an influence of a paramagnetic impurity beyond the detection level of X-ray powder diffraction cannot be ruled out. Phosphorus-31 solid-state magic angle spinning (MAS) NMR spectra of  $W_6PCl_{17}$  reveal a very broad (4700 Hz fwhh) asymmetric isotropic signal at  $\delta = 41$  ppm.

Tungsten atoms in the structure of  $W_6PCl_{17}$  have essentially two types of coordination environments, which can be related to the coordination environments of tungsten atoms in the  $[W_2Cl_9]^{n-}$  ( $n = 2, 3$ ) anion<sup>[19]</sup> and in the  $WCl_4$  structure.<sup>[20]</sup> Nearest W–W distances in  $W_6PCl_{17}$  rank between 2.584(3) and 3.019(4) Å (Table 1) and are very similar to

Table 1. Interatomic distances within the crystal cores of  $W_6PCl_{17}$  and  $W_4(P)Cl_{10}$  in comparison with some other systems.

Compound	M–M distances / Å	W–P distances / Å	P–Cl distances / Å
$W_6PCl_{17}$	2.757(3) [W(1)–W(1)] 3.019(4) [W(1)–W(2) 4×] 2.816(8) [W(2)–W(3) 2×] 2.584(3) [W(3)–W(3)]	2.52(2) [W(1)–P(1) 2×] 2.386(7) [W(2)–P(1) 2×] 2.33(2) [W(3)–P(1) 2×]	
$W_4(P)Cl_{10}$	2.615(1) [W(1)–W(1)] 2.809(1) [W(1)–W(2) 2×] 2.623(1) [W(2)–W(2)]	2.366(4) [W(1)–P(1) 2×] 2.413(4) [W(2)–P(1) 2×]	2.033(8)
$PCl_3$			2.018(3)–2.034(2)
$PCl_5$			1.903(5)–2.16(1)
$W_3(P)(OR)_9$ <sup>[16]</sup>	2.757(1)	2.365(4)	
$W_4(P)_2(OR)_{10}$ <sup>[17]</sup>	2.6938(8) 2.7981(8)	2.292(4) 2.484(4) 2.377(4) 2.692(1)	
$Mo_4Cl_4(OPr)_8$ <sup>[22]</sup>	2.378(2) [Mo(1)–Mo(2)] 2.407(3) [Mo(2)–Mo(2)']		

corresponding distances in *triprismo*-[W<sub>6</sub>ZCl<sub>18</sub>] cluster compounds [2.6518(6)–3.0705(7) Å].<sup>[21]</sup> Likewise, the range of W–P distances between 2.33(2) and 2.52(2) Å is in line with corresponding distances in W<sub>3</sub>(P)(OR)<sub>9</sub> [2.365(4) Å], W<sub>4</sub>(P)<sub>2</sub>(OR)<sub>10</sub> [2.292(4)–2.692(1) Å], and with PCl<sub>3</sub> (Table 1). However, these W–P distances are expectedly longer than the W–Z distances in *triprismo*-[W<sub>6</sub>ZCl<sub>18</sub>] cluster compounds, which typically range between 2.15 and 2.18 Å for Z = C and N.

The complete crystal structure of W<sub>6</sub>PCl<sub>17</sub> features a hexagonal stick packing of halide bridged (W<sub>6</sub>PCl<sub>11</sub>)-Cl<sub>4</sub><sup>a</sup>Cl<sub>4/2</sub><sup>a-a</sup> cluster chains running parallel to the *a* axis (see Figure 2).

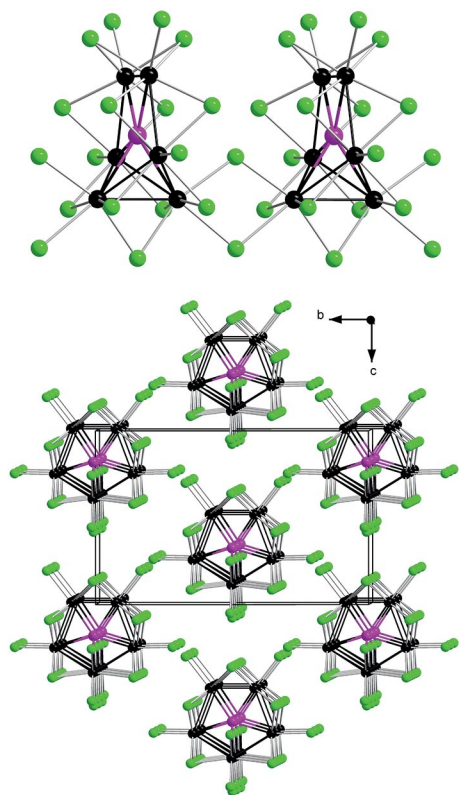


Figure 2. Crystal structure of (W<sub>6</sub>PCl<sub>11</sub>)Cl<sub>4</sub><sup>a</sup>Cl<sub>4/2</sub><sup>a-a</sup> with a section of a cluster chain (top) and a hexagonal stick packing of chains (bottom) running parallel to the *a* axis.

Transition of W<sub>6</sub>PCl<sub>17</sub> into W<sub>4</sub>(PCl)Cl<sub>10</sub> occurs at *T* ≥ 380 °C and can be considered as a reduction because of the presence of excess elemental phosphorus. The crystal structure of W<sub>4</sub>(PCl)Cl<sub>10</sub> features a Jahn–Teller distorted rectangular W<sub>4</sub>-cluster core following the motif of the butadiene structure. Similar clusters were obtained for Mo<sub>4</sub>X<sub>4</sub>(OPr)<sub>8</sub> with X = Cl and Br having planar and butterfly-type Mo<sub>4</sub>-cluster cores, whose individual cluster arrangements were explained simply on the grounds of crystal packing.<sup>[22]</sup> Distances between tungsten atoms within the (nearly) rectangular cluster core of W<sub>4</sub>(PCl)Cl<sub>10</sub> are 2.615(1), 2.623(1), and 2.809(1) Å; intercluster contact distances within the layers of {W<sub>4</sub>(μ<sub>4</sub>-PCl)Cl<sub>6</sub>}Cl<sub>8/2</sub><sup>a-a</sup> are 3.7648(9) and 3.7756(9) Å. Following these contacts, the rectangular clusters are interconnected by bridging chloride

atoms to form a (4<sup>4</sup>) layer structure, displayed in Figure 3. Alternating layers are linked by van der Waals attractions, whereupon empty rectangular spaces within one layer are filled by chloro-phosphinidene ligands of adjacent layers, following a key–lock system.

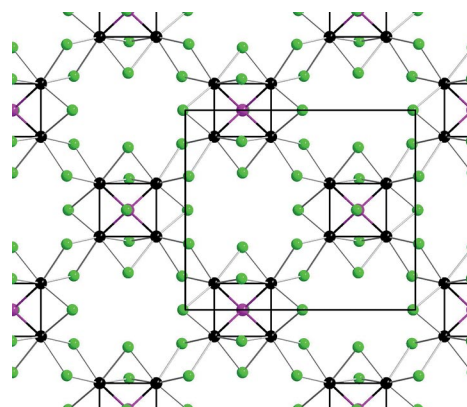


Figure 3. Projection of one layer of the crystal structure of {W<sub>4</sub>(μ<sub>4</sub>-PCl)Cl<sub>6</sub>}Cl<sub>8/2</sub><sup>a-a</sup>.

The most remarkable feature of W<sub>4</sub>(PCl)Cl<sub>10</sub> is the presence of the μ<sub>4</sub>-capping chloro-phosphinidene ligand, having W–P distances of 2.366(4) and 2.413(4) Å, and a P–Cl distance of 2.033(8) Å, which corresponds well with the distances reported for PCl<sub>3</sub>.

Distances within the tungsten cluster cores are listed in Table 1 and can be assigned with the labeling scheme of the cluster cores given in Figure 4.

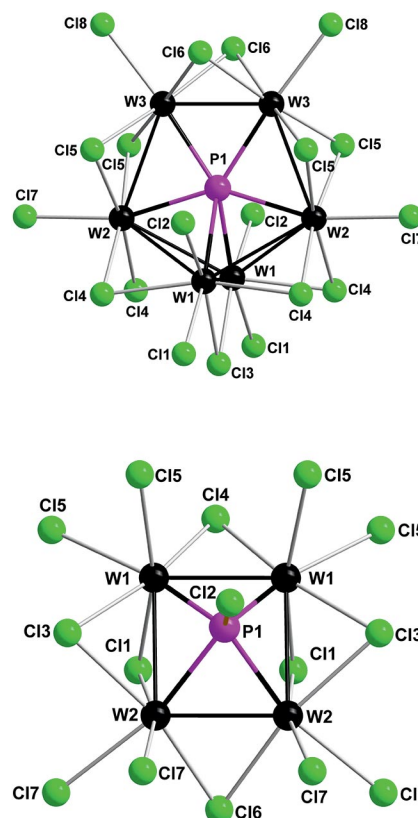


Figure 4. Building blocks from structures of W<sub>6</sub>PCl<sub>17</sub> (top) and W<sub>4</sub>(PCl)Cl<sub>10</sub> (bottom) with atom labels.

In this context, it is interesting to note that a compound containing chlorocarbyne-bridged  $W_2$  units has been reported as  $W_2(\mu_2\text{-CCl})Cl_7$ .<sup>[23]</sup> The chlorocarbyne ligand in this compound is considered as a  $(\text{CCl})^{3-}$  anion, and tungsten atoms are represented as  $W^{5+}$ . The chloro-phosphinidene ligand of  $W_4(\text{PCl})Cl_{10}$  can be treated in an analogous manner and can be considered as a  $(\text{PCl})^{2-}$  anion. This view is consistent with the calculated MO scheme of an isolated  $[W_4(\text{PCl})Cl_{14}]^{4-}$  cluster, which reveals 63 anionic energy levels and 6 metal-based W–W bonding energy levels occupied by 12 electrons (Figure 5). The  $(\text{PCl})$  ligand is represented by eight orbitals ( $2 \times 3s + 6 \times 3p$ ). The covalent P–Cl interaction results in one bonding  $\sigma$  combination below and one antibonding  $\sigma$  combination above the HOMO level. Therefore, the total number of occupied anionic energy levels is  $14 \times 4 (\text{Cl}^-) + 7 (\text{PCl}) = 63$ . The total electron count of 138 valence electrons per  $[W_4(\text{PCl})Cl_{14}]^{4-}$  results in 69 occupied energy levels and 6 occupied metal-centered states.

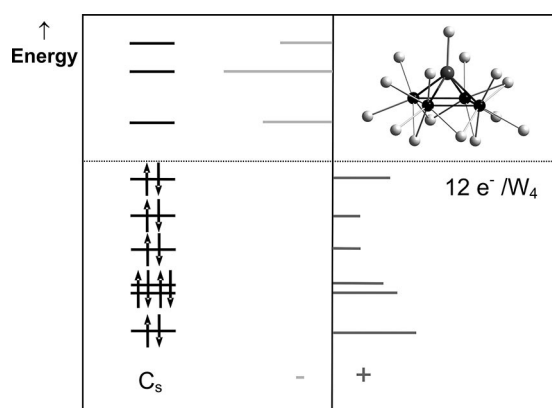


Figure 5. MO scheme of metal-centered states (all a levels) of an isolated  $[W_4(\text{PCl})Cl_{14}]^{4-}$  anion having  $C_s$  symmetry (ideal symmetry:  $C_{2v}$ ) including the bonding (+) and antibonding (–) nature of W–W states.

This cluster electron count and the Jahn–Teller distorted rectangular tungsten cluster core can be related to the electronic situation found in a butadiene molecule or in the cluster core in  $Mo_4Cl_4(\text{OPr})_8$ , and other tetranuclear  $(M_4)^{12+}$  clusters.<sup>[24]</sup> Magnetic measurements on  $W_4(\text{PCl})Cl_{10}$  reveal diamagnetic properties.

The presence of a P–Cl bond in  $W_4(\text{PCl})Cl_{10}$  results in characteristic magnetic-field-dependent splittings as detected in the  $^{31}\text{P}$  MAS NMR spectra (Figure 6a). Analogous splittings have been observed in the  $^{31}\text{P}$  MAS NMR spectra of chloro derivatives of phosphazenes<sup>[25]</sup> and have been analyzed in detail to reveal underlying information on  $^{31}\text{P}$  to  $^{35/37}\text{Cl}$  direct and indirect spin–spin interactions as well as on the  $^{35/37}\text{Cl}$  nuclear quadrupole interactions.<sup>[26]</sup> In the present case, the  $^{31}\text{P}$  to  $^{35}\text{Cl}$  direct dipole–dipole coupling constant has been fixed at 570 Hz and the value calculated from the P–Cl distance and the asymmetry parameter of the electric field gradient tensor about chlorine is assumed to be close to zero and oriented parallel to the P–Cl

bond. With these parameters fixed, the simulation<sup>[27]</sup> (Figure 6a) of the  $^{31}\text{P}$  MAS spectra yields an indirect spin–spin coupling constant  $^1J_{\text{iso}}(^{35}\text{Cl}, ^{31}\text{P})$  of  $-155$  Hz and a  $^{35}\text{Cl}$  nuclear quadrupole coupling constant of  $-50$  MHz. The magnitude of the nuclear quadrupole coupling constant is in line with the proposed correlation between  $^{35}\text{Cl}$  nuclear quadrupole resonance (NQR) frequencies and the P–Cl bond length in chlorocyclotriphosphazatrienes.<sup>[28]</sup> Parameters for the  $^{31}\text{P}$ ,  $^{37}\text{Cl}$  spin pair have been calculated from those of the  $^{31}\text{P}$ ,  $^{35}\text{Cl}$  spin pair by using the ratios of the magnetogyric ratios, 0.8475, or the nuclear quadrupole moments, 0.7874. The  $^{31}\text{P}$  MAS spectrum at 11.75 T also exhibits several spinning sidebands (Figure 6b) caused mainly by chemical shift anisotropy, with principal components of  $\delta_{11} = 406$ ,  $\delta_{22} = 340$ , and  $\delta_{33} = 302$  ppm. In this analysis,

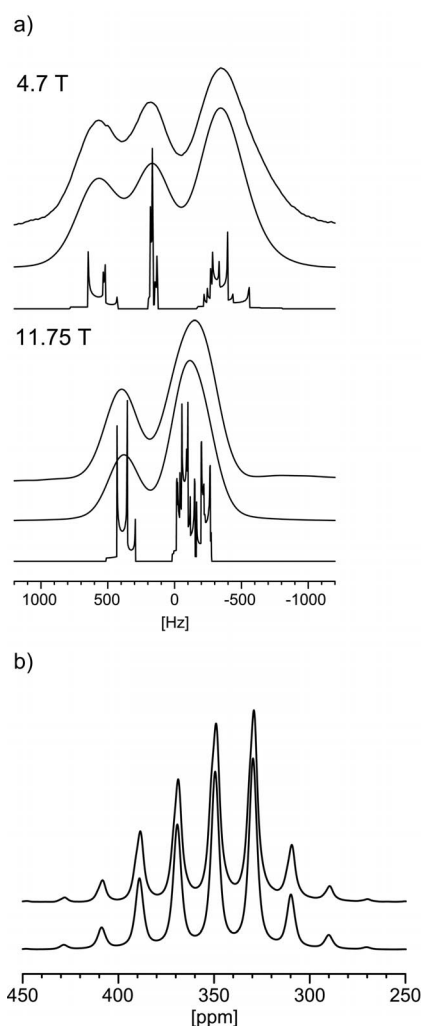


Figure 6. (a) Dependence of the isotropic peak in  $^{31}\text{P}$  MAS spectra of  $W_4(\text{PCl})Cl_{10}$  on external magnetic field strength. For both magnetic field strengths, experimental spectra are shown on top over the convoluted and unconvoluted (bottom) simulated spectra. Frequencies are given relative to the isotropic chemical shift of 349.5 ppm. (b)  $^{31}\text{P}$  MAS NMR spectrum of  $W_4(\text{PCl})Cl_{10}$  at 11.75 T and a spinning rate of 4 kHz. The experimental spectrum (top) was convoluted by a Lorentzian of 500 Hz width to “hide” the fine structure shown in (a). The bottom spectrum was calculated using the  $^{31}\text{P}$  chemical shift anisotropy parameters given in the text.

the  $^{31}\text{P}$  to  $^{35/37}\text{Cl}$  direct dipole–dipole interaction has been neglected. The  $^{31}\text{P}$  isotropic chemical shift of 349.5 ppm is not untypical of phosphinidene units.<sup>[29]</sup>

## Conclusions

The new compounds  $\text{W}_6\text{PCl}_{17}$  and  $\text{W}_4(\text{PCl})\text{Cl}_{10}$  were prepared under moderate heating conditions in order to approach the mostly unexplored field of missing compounds, namely the thermally labile cluster compounds. Their structures comprise phosphido-centered and chlorophosphinidene-capped tungsten clusters, as refined from X-ray diffraction data and confirmed by  $^{31}\text{P}$  NMR spectroscopy. The compounds appear quite stable in air, showing an unchanged powder X-ray diffraction pattern after being exposed to air for one week.

The dimerization of two  $\text{W}_2$  clusters into a  $\text{W}_4$  cluster has been studied by means of solution chemistry<sup>[32]</sup> and appears to be a nice model for the formation of cluster compounds. Following this model, the combination of two  $\text{W}\equiv\text{W}$  dimers leads to the Jahn–Teller distorted tetranuclear cluster with rectangular- or butterfly-shaped  $\text{W}_4$  cluster cores. Both motifs have been reported for  $\text{Mo}_4\text{X}_4(\text{OPr})_8$  clusters with  $\text{X} = \text{Cl}$  and  $\text{Br}$ .<sup>[22]</sup> The planar butadiene-type cluster core is also present in  $\text{W}_4(\text{PCl})\text{Cl}_{10}$ . Upon addition of another  $\text{W}\equiv\text{W}$  dimer to the butterfly-type cluster core, a hexanuclear cluster core is formed, similar to the one that is present in the structure of  $\text{W}_6\text{PCl}_{17}$  (Figure 7).

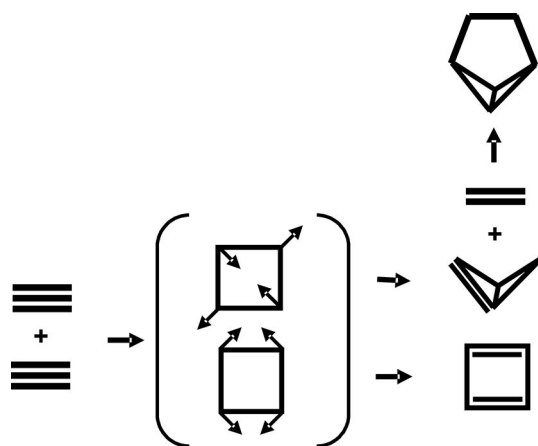


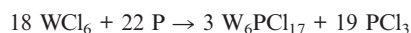
Figure 7. Fragment condensation scheme arising from two  $\text{W}\equiv\text{W}$  dimers forming Jahn–Teller distorted (transition state in parentheses) tetranuclear clusters with a square-planar or butterfly-type cluster core. The addition of another  $\text{W}\equiv\text{W}$  dimer yields the hexanuclear cluster core obtained in the structure of  $\text{W}_6\text{PCl}_{17}$ .

Although the potential of the new compounds remains unknown, it has been shown that metal clusters as well as metal surfaces often reveal common modes of substrate binding and may provide special properties. This may be challenging in the case of the chloro-phosphinidene ligand, which is situated on rectangular crystal faces of air-stable  $\text{W}_4(\text{PCl})\text{Cl}_{10}$ .

## Experimental Section

**Syntheses:** Reactions between  $\text{WCl}_6$  and an approximately threefold molar excess of elemental red phosphorus were performed in silica tubes between 200 and 600 °C in intervals of 10 °C. After the compositions of the new products were identified by XRD methods, compositions of the starting materials were adjusted as follows.

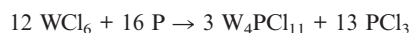
**$\text{W}_6\text{PCl}_{17}$ :**  $\text{WCl}_6$  (150 mg, 0.38 mmol; Aldrich, 99.9%) and elemental red P (15.7 mg, 0.51 mmol; Aldrich, 99%) were mixed under an argon atmosphere (glovebox), sealed in an evacuated silica tube, and then heated in a tube furnace for 24 h at 370 °C. The following reaction is assumed:



The black microcrystalline powder was removed from the ampoule and purified by subliming off the coproduced  $\text{PCl}_3$  to give an estimated yield (from XRD) of 95%  $\text{W}_6\text{PCl}_{17}$ .

The X-ray powder pattern of a single-phase sample was indexed, and the crystal structure was solved with the program EXPO<sup>[30]</sup> by using direct methods and structure refinements with Winplotr (Fullprof).<sup>[31]</sup>

**$\text{W}_4\text{PCl}_{11}$ :**  $\text{WCl}_6$  (150 mg, 0.38 mmol; Aldrich, 99.9%) and elemental red P (15.7 mg, 0.51 mmol; Aldrich, 99%) were mixed under an argon atmosphere (glove box), sealed in an evacuated silica tube, and then heated in a tube furnace for 24 h at 500 °C. The following reaction is assumed:



The product contained black platelike crystals of  $\text{W}_4\text{PCl}_{11}$ , small amounts of needlelike  $\text{WCl}_4$  crystals (<5%) that were located at one end of the silica tube, and  $\text{PCl}_3$ . After  $\text{PCl}_3$  was sublimed off, the product contained an estimated yield (from XRD) of 95%  $\text{W}_4\text{PCl}_{11}$ . A single crystal of  $\text{W}_4\text{PCl}_{11}$  was selected for X-ray structure refinement.

The compounds  $\text{W}_6\text{PCl}_{17}$  and  $\text{W}_4(\text{PCl})\text{Cl}_{10}$  show an unchanged powder X-ray pattern after exposure to air for one week.

A transition from  $\text{W}_6\text{PCl}_{17}$  into  $\text{W}_4\text{PCl}_{11}$  occurs with the presence of excess elemental phosphorus when heating near or above 380 °C. The following reaction is assumed:



**Powder X-ray Diffraction:**  $\text{W}_6\text{PCl}_{17}$ ,  $M_r = 1736.77 \text{ g mol}^{-1}$ , orthorhombic space group  $Imm2$ ,  $a = 6.7835(2) \text{ \AA}$ ,  $b = 15.8762(3) \text{ \AA}$ ,  $c = 10.0727(2) \text{ \AA}$ ,  $V = 1084.79 \text{ \AA}^3$ ,  $F(000) = 1496$ ,  $\rho_{\text{calcd.}} (Z = 2) = 5.31679 \text{ g cm}^{-3}$ ,  $\theta$  range = 2.5–60°,  $\text{Cu-K}\alpha_1$  ( $\lambda = 1.54060 \text{ \AA}$ ),  $T = 293(2) \text{ K}$ , 509 measured data (STOE StadIP). Structure solution by direct methods (EXPO 2009), structure refinement by global refinement (FullProf Suite), data to parameter ratio: 11.8:1, final  $R$  indices:  $R_p = 0.0522$ ,  $R_{wp} = 0.0693$ ,  $R_{\text{Bragg}} = 0.0673$ ,  $\chi^2 = 2.8613$ .

**Single-Crystal X-ray Diffraction:**  $\text{W}_4(\text{PCl})\text{Cl}_{10}$ ,  $M_r = 1156.32 \text{ g mol}^{-1}$ , monoclinic space group  $C2/m$ ,  $a = 13.257(3) \text{ \AA}$ ,  $b = 9.850(2) \text{ \AA}$ ,  $c = 11.400(2) \text{ \AA}$ ,  $\beta = 91.38(2)^\circ$ ,  $V = 1488.2(5) \text{ \AA}^3$ ,  $F(000) = 1992$ ,  $\rho_{\text{calcd.}} (Z = 4) = 5.161 \text{ g cm}^{-3}$ ,  $\mu = 32.863 \text{ mm}^{-1}$ , approximate crystal dimensions  $0.14 \times 0.1 \times 0.04 \text{ mm}^{-1}$ ,  $\theta$  range = 2.58–25.97°,  $\text{Mo-K}\alpha$  ( $\lambda = 0.71073 \text{ \AA}$ ),  $T = 293(2) \text{ K}$ , 5240 measured data (STOE IPDS) of which 1524 ( $R_{\text{int}} = 0.1162$ ) unique; Lorentz and polarization correction (STOE IPDS Software), absorption correction (X-Red/X-Shape). Structure solution by direct methods (SHELX-97), full-matrix least-squares refinement on  $F^2$ , data to parameter ratio: 19.3:1, final  $R$  indices: [ $I > 2\sigma(I)$ ]:  $R1 = 0.0438$ ,  $wR2 = 0.0693$ ,  $R$  indices (all data):  $R1 = 0.0737$ ,  $wR2 = 0.0773$ , GOOF on  $F^2 = 0.895$ .

**Magnetic Measurements:** Magnetic susceptibility measurements were performed in gelatine capsules with a SQUID magnetometer (Quantum Design, MPMS) in the temperature range between 300 and 1.8 K.

**Solid-State NMR Spectroscopy:** Solid-state  $^{31}\text{P}$  magic-angle spinning (MAS) spectra were acquired at 4.7 T by using a Bruker DSX-200 wide-bore spectrometer equipped with a double-bearing broadband cross-polarization (CP)/MAS probe head operating at 81.01 MHz for  $^{31}\text{P}$ , and at 11.75 T by using a Bruker Avance II+500 standard-bore spectrometer equipped with a HR-MAS probe head operating at 202.46 MHz. Samples were packed into 4-mm (o.d.) zirconia rotors sealed with Kel-F caps. Spectra were acquired after single-pulse excitation under the following spinning frequencies, recycle delays, and number of scans: 8 kHz, 200 s, 330 scans (4.7 T); 4 kHz, 60 s, 4300 scans (11.75 T).  $^{31}\text{P}$  chemical shifts are reported with respect to external 85% aqueous phosphoric acid. Spectral simulations were carried out by using WSolid1.<sup>[27]</sup>

Further details on the crystal structure investigation(s) may be obtained from the Fachinformationszentrum Karlsruhe, 76344 Eggenstein-Leopoldshafen, Germany (Fax: +49-7247-808-666; E-mail: crysdata@fiz-karlsruhe.de), on quoting the depository numbers CSD-422270 for  $\text{W}_6\text{PCL}_{17}$  and CSD-422269 for  $[\text{W}_4(\text{PCL})\text{Cl}_{10}]$ .

## Acknowledgments

The authors would like to thank Prof. Dr. J. Köhler and Dr. R. K. Kremer from the MPI in Stuttgart for the magnetic measurements.

- [1] a) T. G. Gray, *Chem. Eur. J.* **2009**, *15*, 2581–2593; b) M. Ströbele, T. Jüstel, H. Bettentrup, H.-J. Meyer, *Z. Anorg. Allg. Chem.* **2009**, *635*, 822–827; c) D. G. Nocera, H. B. Gray, *J. Am. Chem. Soc.* **1984**, *106*, 824–825.
- [2] S. Kamiguchi, S. Nagashima, K. Komori, M. Kodomari, T. Chihara, *J. Cluster Sci.* **2007**, *18*, 414–430.
- [3] a) D. J. Osborn, G. L. Baker, R. N. Ghosh, *J. Sol-Gel Sci. Technol.* **2005**, *36*, 5–10; b) R. N. Ghosh, G. L. Baker, C. Ruud, D. G. Nocera, *Appl. Phys. Lett.* **1999**, *75*, 2885–2887.
- [4] a) R. Siepmann, H. G. von Schnering, H. Schäfer, *Angew. Chem.* **1967**, *79*, 650; b) A. Nägele, J. Glaser, H.-J. Meyer, *Z. Anorg. Allg. Chem.* **2001**, *627*, 244–249; c) S. Tragl, J. Glaser, C. Vincent, R. Llusar, H.-J. Meyer, *Inorg. Chem.* **2009**, *48*, 3825–3831.
- [5] Y.-Q. Zheng, H. G. von Schnering, J. H. Chang, Y. Grin, G. Engelhardt, G. Heckmann, *Z. Anorg. Allg. Chem.* **2003**, *629*, 1256–1264.
- [6] a) H. Womelsdorf, H.-J. Meyer, *Angew. Chem.* **1994**, *106*, 2022–2023; *Angew. Chem. Int. Ed. Engl.* **1994**, *33*, 1943–1944; b) H. Womelsdorf, H.-J. Meyer, *Z. Anorg. Allg. Chem.* **1996**, *622*, 2083–2088.
- [7] a) E. J. Welch, N. R. M. Crawford, R. G. Bergmann, J. R. Long, *J. Am. Chem. Soc.* **2003**, *125*, 11464–11465; E. J. Welch, C. L. Yu, N. R. M. Crawford, J. R. Long, *Angew. Chem.* **2005**, *117*, 2605–2609; *Angew. Chem. Int. Ed.* **2005**, *44*, 2549; b) E. J. Welch, J. R. Long, *Prog. Inorg. Chem.* **2005**, *54*, 1–45.
- [8] E. J. Welch, J. R. Long, *Angew. Chem.* **2007**, *119*, 3564–3566; *Angew. Chem. Int. Ed.* **2007**, *46*, 3494–3496.
- [9] R. E. McCarley, T. M. Brown, *Inorg. Chem.* **1964**, *3*, 1232–1236.
- [10] a) V. Kolesnichenko, L. Messerle, *Inorg. Chem.* **1998**, *37*, 3660–3663; b) M. Ströbele, T. Jüstel, H. Bettentrup, H.-J. Meyer, *Z. Anorg. Allg. Chem.* **2009**, *635*, 822–827; c) M. Ströbele, H.-J. Meyer, *Z. Anorg. Allg. Chem.* **2009**, *635*, 1517–1519.
- [11] M. Ströbele, H.-J. Meyer, *Inorg. Chem.* **2010**, *49*, 5986–5991.
- [12] M. Ströbele, H.-J. Meyer, *Z. Anorg. Allg. Chem.* **2010**, *636*, 62–66.
- [13] G. I. Novikov, N. V. Andreeva, O. G. Polyachenok, *Russ. J. Inorg. Chem.* **1961**, *6*, 1990–1993.
- [14] V. Kolesnichenko, D. Swenson, L. Messerle, *Inorg. Chem.* **1998**, *37*, 3257–3262.
- [15] G. Rosenthal, J. D. Corbett, *Inorg. Chem.* **1988**, *27*, 53–56.
- [16] M. H. Chisholm, K. Folting, J. W. Pasterczyk, *Inorg. Chem.* **1988**, *27*, 3057.
- [17] M. H. Chisholm, K. Folting, M. Scheer, *Polyhedron* **1998**, *17*, 2931–2935.
- [18] C. Mealli, D. Proserpio, *J. Chem. Educ.* **1990**, *67*, 399–402.
- [19] R. Stranger, S. A. Macgregor, T. Lovell, J. E. McGrady, G. A. Heath, *J. Chem. Soc., Dalton Trans.* **1996**, 4485–4491.
- [20] A. Nägele, Dissertation, Univ. Tübingen, **2001**.
- [21] M. Weisser, R. Burgert, H. Schnöckel, H.-J. Meyer, *Z. Anorg. Allg. Chem.* **2008**, *634*, 633–640.
- [22] M. H. Chisholm, D. L. Clark, R. J. Errington, K. Folting, J. C. Huffmann, *Inorg. Chem.* **1988**, *27*, 2071–2084.
- [23] J. Beck, F. Wolf, *Z. Anorg. Allg. Chem.* **2002**, *628*, 1453–1454.
- [24] B. E. Bursten, M. H. Chisholm, D. L. Clark, *Inorg. Chem.* **1988**, *27*, 2084–2096.
- [25] a) S. Paasch, K. Krüger, B. Thomas, *Solid State Nucl. Magn. Reson.* **1995**, *4*, 267–280; b) N. C. Gonnella, C. Busacca, S. Campbell, M. Eriksson, N. Grinberg, T. Bartholomeyzik, S. Ma, D. L. Norwood, *Magn. Reson. Chem.* **2009**, *47*, 461–464.
- [26] a) B. Thomas, S. Paasch, S. Steuernagel, K. Eichele, *Solid State Nucl. Magn. Reson.* **2001**, *20*, 108–117; b) A. Rabis, A.-R. Grimmer, B. Thomas, E. Brendler, S. Beck, M. Meisel, *Solid State Nucl. Magn. Reson.* **2005**, *28*, 57–63.
- [27] K. Eichele, R. E. Wasylshen, *WSolids1 ver. 1.20.4*, University of Tübingen and Dalhousie University, HaliFax, **2010**.
- [28] A. Connelly, W. H. Dalglish, P. Harkins, R. Keat, A. L. Porte, I. Raitt, R. A. Shaw, *J. Magn. Reson.* **1978**, *30*, 439–450.
- [29] K. Eichele, R. E. Wasylshen, J. F. Corrigan, N. J. Taylor, A. J. Carty, *J. Am. Chem. Soc.* **1995**, *117*, 6961–6969.
- [30] A. Altomare, M. Camalli, C. Cuocci, C. Giacobozzo, A. Moliterni, R. Rizzi, *J. Appl. Crystallogr.* **2009**, *42*, 1197–1202.
- [31] T. Roisnel, J. Rodriguez-Carvajal, *WinPLOTR: A Windows Tool for Powder Diffraction Pattern Analysis. Proceedings of the Seventh European Powder Diffraction Conference (EPDIC 7)* (Eds. R. Delhez, E. J. Mittenmeijer), **2000**, 118.
- [32] M. Chisholm, C. E. Hammond, M. Hampden-Smith, J. C. Huffman, W. G. v. d. Sluys, *Angew. Chem.* **1987**, *99*, 937–939.

Received: February 4, 2011

Published Online: May 26, 2011